

# Calibration of $V_s$ -based empirical models for assessing soil liquefaction potential using expanded database

Chen Guoxing<sup>1,2</sup> · Kong Mengyun<sup>1,2</sup> · Sara Khoshnevisan<sup>3</sup> · Chen Weiyun<sup>1,2</sup> · Li Xiaojun<sup>1,4</sup>

Received: 20 April 2017 / Accepted: 5 August 2017 / Published online: 19 August 2017  
© Springer-Verlag GmbH Germany 2017

**Abstract** The shear wave velocity ( $V_s$ )-based method of assessing the liquefaction susceptibility of soils has given geotechnical engineers a promising alternative for determining soil resistance to seismic liquefaction. Through the use of an expanded global case histories of soil liquefaction, the authors obtained a new calibrated correlation equation for liquefaction triggering analysis. This new liquefaction triggering correlation was found to be reasonably conservative, and yet insensitive to the variations in the components of the adopted simplified analysis framework. A probabilistic version of the liquefaction triggering correlation, obtained with the weighted maximum-likelihood technique, was validated using a

weighted empirical probability approach. Three zones of liquefaction potential, transitioning from non-liquefaction to liquefaction, were then defined based on liquefaction probability contours.

**Keywords** Soil liquefaction · Probability · Shear wave velocity · Case history

## Introduction

The widespread liquefaction phenomena in loose saturated sandy sediments is an inevitable occurrence in coastal plains subjected to great earthquakes. For example, severe liquefaction occurred in the Tianjing coastal plain during the 1976 Tangshan  $M_w$  7.6 earthquake (Fu and Tatsuoka 1984; Liu 1986), the Hanshin area during the 1995 Hyogo-ken Nanbu  $M_w$  6.9 earthquake (Elgamal et al. 1996), the eastern suburbs and satellite townships of Christchurch, New Zealand during the 2010–2011 Canterbury  $M_w$  5.2–7.1 earthquake sequence (Quigley et al. 2013), and the reclaimed shore areas of Tokyo Bay during the 2011  $M_w$  9.0 earthquake off the Pacific coast of Tohoku (Bhattacharya et al. 2011; Yamaguchi et al. 2012).

The effect of soil liquefaction in an earthquake can be devastating. For example, the 2011 Tohoku Earthquake off the Pacific Coast also indirectly resulted in the radioactive contamination of the surface from the accident at the Fukushima Daiichi nuclear power plant. Similarly, although the reactors of the Kashiwazaki-Kariwa nuclear power plant were safely shut down during the 2007 Niigata Chuetsu-offshore  $M_w$  6.8 earthquake off the coast of Japan, damage nonetheless occurred, and the subsequent soil liquefaction severely affected the structures, triggered a transformer fire, and simultaneously damaged the fire-suppression system and closed the wastewater treatment facility (RGHNCE 2008). These events clearly

## Highlights

1. A new  $V_s$ -based deterministic liquefaction triggering correlation was determined
2. The new correlation is insensitive to variations in the components of liquefaction analysis framework
3. An empirical equation for determining the probability of liquefaction was determined
4. A probabilistic version of the new calibrated liquefaction triggering correlation is presented

✉ Chen Guoxing  
gxc6307@163.com

Sara Khoshnevisan  
khoshnevisan.sara@gmail.com

- <sup>1</sup> Institute of Geotechnical Engineering, Nanjing Tech University, Nanjing 210009, China
- <sup>2</sup> Civil Engineering and Earthquake Disaster Prevention Center of Jiangsu Province, Nanjing 210009, China
- <sup>3</sup> Civil and Environmental Engineering Department, Clarkson University, Potsdam, NY 13699, USA
- <sup>4</sup> Institute of Geophysics, China Earthquake Administration, Beijing 100081, China

indicate the vulnerability of nuclear power plants located in coastal plains from tremendous original and secondary disasters induced by seismic soil liquefaction. Thus, designing facilities against such devastating geotechnical and geo-environmental issues from great earthquakes in coastal areas has presented a huge challenge to geotechnical engineers and designers. In practice, the engineer generally adopts simplified methods for assessing liquefaction potential and risk at a given project site.

The simplified method, pioneered by Seed and Idriss (1971), is the most widely adopted method for evaluating the seismic soil liquefaction potential in North America and throughout much of the world. This method is used to determine soil liquefaction resistance at a given depth of a soil profile subjected to the earthquake loading expressed as cyclic stress ratio ( $CSR$ ) (e.g., Seed 1979, 1987; Seed et al. 1985; Idriss 1999; Cetin et al. 2002, 2004; Youd et al. 2001; Idriss and Boulanger 2006, 2008, 2010; Boulanger and Idriss 2012). The main task of the liquefaction evaluation involves determination of the cyclic resistance ratio ( $CRR$ ), i.e., the capacity of the soil to resist seismic liquefaction, using in situ tests such as the standard penetration test (SPT), the cone penetration test (CPT), and the shear-wave velocity ( $V_s$ ) measurement. Although the SPT, the CPT, and the  $V_s$  measurement can all be used to assess the  $CRR$  and the liquefaction potential, only the latter is focused on in this paper.

Unlike the SPT and CPT penetration methods,  $V_s$  actually measures the fundamental property of the soil and is considerably less sensitive to the problems of soil compression and penetration resistance reduction in the presence of fine soils (Kayen et al. 2013). It is also more suitable for sites underlain by soils that are difficult to penetrate or sample (Andrus and Stokoe 2000; Kayen et al. 2013). Although not as widely adopted as the SPT-based and CPT-based methods, the  $V_s$ -based simplified method for the liquefaction potential evaluation has gained significant attention in the geotechnical earthquake engineering communities (e.g., Dobry et al. 1982; Alba et al. 1984; Tokimatsu and Uchida 1990; Kayen et al. 1992; Robertson et al. 1992; Lodge 1994; Andrus and Stokoe 2000; Juang et al. 2001; Youd et al. 2001; Juang et al. 2002a; Andrus et al. 2004; Chen et al. 2005; Juang et al. 2005; Liu and Mitchell 2006; Zhou and Chen 2007; Uyanik and Taktak 2009; Zhou et al. 2010; Kayen et al. 2013; Ahmadi and Paydar 2014; Dobry et al. 2015).

Juang et al. (2002a) presented a probability-based method for their evaluation of liquefaction potential using  $V_s$ . Based on the Bayesian mapping functions developed by Juang et al. (2002a), a factor of safety against liquefaction of  $F_s = 1.2$  obtained with the  $V_s$ -based method of Andrus and Stokoe (2000) corresponds to an expected liquefaction probability of 16%. Similarly, Kayen et al. (2013) recommended the adoption of a probability of liquefaction of  $P_L = 15\%$ , which corresponds to  $F_s = 1.17$  in their calibration study, for use as

the single deterministic boundary curve for evaluating the liquefaction potential.

Kayen et al. (2013) compiled a global database of 415  $V_s$ -based case histories of field liquefaction performance in an effort to better define the boundary curve at high  $CSR$  values. They concluded that there was no need to artificially set a limiting upper bound of the effective overburden stress-corrected shear wave velocity of clean soils ( $V_{s1}$ ). This limiting upper bound of the  $V_{s1}$  had previously been assumed to vary from 200 m/s for soils with a fine content of 35% to 215 m/s for soils with a fine content of 5% or less at liquefaction sites (Andrus and Stokoe 2000; Youd et al. 2001).

Figure 1 compared the liquefaction triggering correlations of clean sands from the 15% probability contour developed by Kayen et al. (2013), and the 10% and 50% probability contour developed by Juang et al. (2002a), against the deterministic boundaries developed by Andrus and Stokoe (2000), and the lower boundaries developed by Zhou and Chen (2007). Although the liquefaction triggering correlation developed by Kayen et al. (2013) may be useful in civil engineering projects with low-to-medium potential risk, it appears less suitable for critical infrastructures such as nuclear power plants. Therefore, it is necessary to re-calibrate the liquefaction triggering correlations using the expanded  $V_s$ -based case history database to reduce the probability of mistaking liquefiable soil for non-liquefiable soil when evaluating the liquefaction potential for projects with different risk levels.

In this paper, a new empirical liquefaction triggering correlation is obtained through an updated calibration using an expanded database, and a conservative assessment procedure is established for evaluation of the soil liquefaction potential at nuclear power plant project sites with extremely high-risk potential. Then, a simplified probabilistic version of the proposed correlation, expressed in terms of the  $P_L$  and the nominal safety factor ( $\tilde{F}_s$ ), is presented. It should be noted that the nominal value of the safety factor was defined as the ratio of the nominal cyclic resistance ratio ( $\widetilde{CRR}$ ) over the nominal cyclic stress ratio ( $\widetilde{CSR}$ ), following the probability-based analysis framework developed by Juang et al. (2012, 2013).

## Calibration of the new liquefaction triggering correlation based on expanded database

### Case history database

The  $V_s$ -based liquefaction and non-liquefaction case history database in this paper has been expanded from the databases of Andrus et al. (1999), Chu et al. (2004), Saygili (2005), and Kayen et al. (2013). These data were combined into a global catalog of 618 case histories from 49 earthquake events with  $V_s$ -based liquefaction performance observations, of which 380

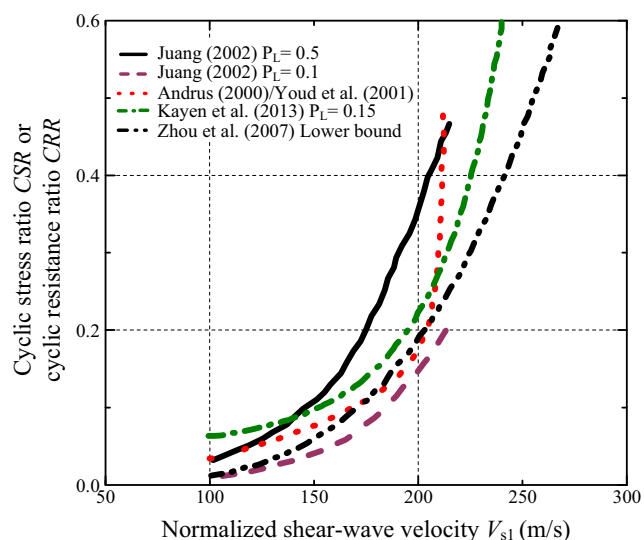


**Fig. 1** Comparison of the liquefaction triggering correlation ( $M_w = 7.5$ ) for the deterministic  $V_s$ -based assessment of liquefaction for clean sand

cases exhibited surface evidence of liquefaction, 234 cases exhibited no surface evidence of liquefaction, and four cases from 2003 Tokachi Oki  $M_w$  7.8 earthquake were in the margin between liquefaction and non-liquefaction. In general, the occurrence of ground failure at the surface (e.g., hydraulic fracturing, sand boiling, ground cracking, lateral spreading or sliding) and its resulting effects (e.g., the uplifting of the manholes and sewage drainage pipes, the settling and tilting of the buildings and houses) were observed at the liquefaction sites. The contents of these expanded databases are detailed below.

Of the 12 case history data developed by Chu et al. (2004) from the 1999 Chi-Chi, Taiwan  $M_w$  7.6 earthquake, nine cases indicated surface evidence of liquefaction, three cases indicated no evidence of surface liquefaction, and one case was in the realm between liquefaction and non-liquefaction (called marginal cases). Of the 41 case histories developed by Saygili (2005) from the 1999 Chi-Chi earthquake and the 1999 Kocaeli, Turkey  $M_w$  7.4 earthquake, 24 cases indicated surface evidence of liquefaction, and 17 cases indicated no surface evidence of liquefaction. Of the 415 case histories developed by Kayen et al. (2013) from the earthquakes in Mainland China, Greece, Japan, Taiwan (China), and the United States, 287 cases indicated a surface evidence of liquefaction, 124 cases indicated no surface evidence of liquefaction, and four cases were marginal cases. Of the 225 case histories developed by Andrus et al. (1999) from earthquakes in Mainland China, Japan, Taiwan (China), and the United States, 75 cases were the same as those developed by Kayen et al. (2013) and were removed from the final database. Thus, only 150 cases from the database by Andrus et al. (1999) were included in the final database. Of these 150 cases, 60 indicated a surface evidence of liquefaction and 90 indicated no surface evidence of liquefaction.

In summary, the final database included 380 liquefaction cases and 234 no-liquefaction cases for a total of 614 case histories from 49 earthquakes. The details of the final database are presented in Table 1.

### Normalized shear-wave velocity and effect of fines content

The shear wave velocity ( $V_s$ ) is a small-strain property related to the undisturbed shear modulus and the mass density of the soil. The  $V_s$  of a soil is primarily influenced by the principal stresses in the direction of wave propagation and particle motion, and soil conditions, such as void ratio, stress history, grain characteristics, cementation, and geologic age (Andrus and Stokoe 2000; Ahmadi and Paydar 2014). Of course, the measurement accuracy and precision of  $V_s$  depends on geophysical test methods, procedural details, soil conditions, and interpretation technique. The uncertainties associated with the calculation of the dispersion curve and the inversion of individual shear-wave velocity profiles were beyond the scope of this study, and will be elucidated in future work. A study by Moss (2008) indicates that the average combined coefficient of variation for the dispersion and inversion calculations of the test data of spectral-analysis-of-surface-waves is approximately 0.15. Typically, the field measurement of  $V_s$  is corrected to a normalized  $V_{s1}$  at a reference stress of 100 kPa as follows (Kayen et al. 1992; Robertson et al. 1992; Andrus et al. 2004):

$$V_{s1} = V_s \left( \frac{P_a}{\sigma_v} \right)^{0.25} \quad (1)$$

Three methods are available to assess the effect of the fines content ( $FC$ ): (1) the use of inter-granular soil mechanics, (2) the undertaking of field SPT and CPT penetration measurements, and (3) the use of  $V_s$  for low-strain measurements (Kayen et al. 2013). For penetration measurements, the increase of the non-plastic fines causes the apparent decrease of the frictional resistance and increases excess pore pressures. As such, the effect of  $FC$  as applied to the penetration-based liquefaction correlation boundaries is quite strong (Polito 1999). On the other hand, the  $V_s$  measurement is non-invasive and it measures the small strain shear modulus  $G_0$  through  $V_s$  [ $G_0 = \rho V_s^2$ , where  $\rho$  is the mass density of soil]. Given the very small difference between the  $G_0$  of sand and silty or clayey sand, all these soils exhibit the same initial stiffness when undergoing strain (Iwasaki and Tatsuoka 1977), which renders the  $V_s$  measurements relatively insensitive to any small discrepancies in the  $FC$ . The work of Kayen et al. (2013) on the liquefaction correlation boundary curve shows that the required adjustment of  $V_s$  to account for the effect of  $FC$  (from 5% to 35%) is generally less than 5 m/s. This is quite consistent with the findings of previous studies (Andrus and Stokoe 2000; Huang et al. 2004; Liu and Mitchell 2006; Zhou and Chen 2007; Dabiri et al. 2011).

**Table 1** Basic information of liquefaction databases from  $V_s$  case history data

No	Earthquake event, occurrence date and magnitude	PGA (g)	CSR	Number of liquefied sites?		Liquefaction critical depth range (m)	GWT Depth (m)	$V_s$ (m/s)	Cited reference
				Liq.	No liq.				
1	1906 San Francisco, $M_w$ 7.7	0.32–0.36	0.240–0.288	1	1	4.75–9.85	2.4–6	172.0–172.1	Kayen et al. (2013)
2	1948 Fukui, $M_w$ 7.1	0.5	0.305–0.492	10	1	1.1–9.5	0.5–1.3	134–312.5	
3	1968 Tokachi Oki, $M_w$ 7.9	0.15–0.23	0.177–0.257	5	0	2.75–6.5	0.8–1	109.9–148.5	
4	1973 Miyagi Ken Oki, $M_w$ 7.4	0.2–0.32	0.160–0.346	10	1	3–9	0.5–2.7	110.2–171.8	
5	1976 Tangshan, $M_w$ 8.0	0.2–0.45	0.163–0.566	16	8	1.35–8.15	0.7–3.7	140.9–336.6	
6	1978 Miyagi Ken Oki, $M_w$ 6.7	0.12–0.14	0.078–0.105	2	6	4.3–7.5	0.5–2.6	140.9–172.2	
7	1983 Nihonkai Chubu, $M_w$ 7.7	0.12–0.28	0.133–0.335	8	0	4–7.075	0.4–1.5	123.4–184.2	
8	1983 Nihonkai Chubu, $M_w$ 7.0, Aftershock	0.12	0.107–0.117	2	0	4.4–6	0.4–1.0	123.4–139	
9	1986 Lotung LSST, $M_w$ 6.6,6	0.04–0.18	0.025–0.136	0	6	3.5	0.5	159.2	
10	1986 Chiba-Ibaragi-Kenkyo, $M_w$ 6	0.06	0.032–0.038	0	2	6.15–14.8	1.4	152.7–153.8	
11	1989 Loma Prieta, $M_w$ 7	0.11–0.47	0.062–0.375	42	17	2.15–9.85	0.6–6.4	124–239.6	
12	1993 Kushior, $M_w$ 7.6	0.4–0.46	0.260–0.433	8	0	2.55–9	1.0–2.0	118.5–197.6	
13	1993 Hokkaido Nansai Oki, $M_w$ 7.7	0.14–0.50	0.104–0.591	24	3	1.45–7.5	0.5–3	81.7–213	
14	1995 Hyogo Nambu, $M_w$ 7	0.12–0.60	0.097–0.554	67	18	2.5–18.5	0.5–7	124.3–298.2	
15	1999 Chi Chi, $M_w$ 7.6	0.25–0.70	0.258–0.688	13	1	2.15–12.7	0.5–3	147.4–217.8	
16	1999 Druce, $M_w$ 7.4	0.4	0.341–0.356	2	0	7.25–7.5	2.4	137.3–146.7	
17	2000 Tottori Seibu, $M_w$ 6.8	0.33–0.38	0.231–0.319	3	0	5.6–6.0	1.0–2	100.1–129.5	
18	2001 Geiyo Hiroshima, $M_w$ 6.8	0.25–0.26	0.147–0.211	5	0	2.5–10.5	1.0–3.0	145.9–9.3	
19	2002 Denali Fault, $M_w$ 7.9, 7	0.36–0.39	0.231–0.374	4	5	1.75–2.35	0.5–1	149.1–362.9	
20	2003 Sanriku Minami, $M_w$ 7	0.22–0.28	0.147–0.227	2	9	3.0–9.0	0.5–2.7	110.2–172.2	
21	2003 Tokachi Oki, $M_w$ 7.8	0.09–0.4	0.103–0.447	3	3	4.5–9.0	1.0–2	109.9–197.6	
22	2003 Tokachi Oki, $M_w$ 7.1, Aftershock	0.13	0.120	0	1	6.5	1.0	109.9	
23	2007 Niigata Chuetsu Oki, $M_w$ 6.6	0.68	0.598–0.637	2	0	3.5–5.0	2.4	136.7–157.8	
24	2008 Achaia Elia, $M_w$ 6.5	0.33	0.256–0.285	2	0	5.5	2.4	191.0–193.4	
25	2011 Tohoku, $M_w$ 9.0, Mainshock	0.27	0.328–0.353	2	0	4.55–4.6	2.4	139.0–139.5	
26	2011 Tohoku, $M_w$ 7.4, Aftershock	0.2–0.76	0.210–0.676	10	0	2.9–9.0	2.4	111.1–172.7	
27	1964 Niigata, $M_w$ 7.5	0.16–0.18	0.103–0.193	6	3	3.6–10.5	1.2–5	122.2–170.6	Kayen et al. (2013);
28	1975 Haicheng, $M_w$ 7.1	0.12	0.105–0.118	5	1	1.9–10.25	0.5–1.5	101.3–152.1	Andrus et al. (1999)
29	1979 Imperial Valley, $M_w$ 6.5	0.12–0.51	0.066–0.329	4	7	3–4.65	1.4–2.7	98.3–203.9	
30	1980 Mid Chiba, $M_w$ 5.9	0.08	0.047–0.050	0	2	6.15–14.8	1.4	152.7–153.8	
31	1981 Westmorland, $M_w$ 5.9	0.02–0.36	0.008–0.175	6	5	3.15–4.65	1.4–2.7	98.3–203.9	
32	1983 Bora Peak, $M_w$ 6.9	0.23–0.5	0.146–0.416	20	4	2–3.65	0.8–3	114.9–328.6	
33	1987 Chiba-Toho-Oki, $M_w$ 6.5	0.1	0.048	0	1	9.1	6.2	110.8	
34	1987 Superstition Hills, $M_w$ 6.5	0.15–0.2	0.066–0.140	3	8	3.15–4.65	1.4–2.7	99.4–211.7	
35	1987 Elmore Ranch, $M_w$ 5.9	0.03–0.15	0.012–0.073	0	11	3.15–4.65	1.4–2.7	98.3–211.7	
36	1906 San Francisco, $M_w$ 7.7	0.32–0.36	0.214–0.293	8	4	4.2–9.9	2.4–6.1	124–191	Andrus et al. (1999)
37	1957 Daly City, $M_w$ 5.3	0.11	0.349–0.449	0	5	3.5–7.9	2.7–5.9	113–211	
38	1985 Chiba Ibaragi, $M_w$ 6	0.05	0.028–0.03	0	2	6.1–14.1	1.3	173–185	
39	1985 Taiwan (event Lss2), $M_w$ 5.3	0.05	0.037	0	4	5.3–6.1	0.5	155–191	
40	1985 Taiwan (event Lss3), $M_w$ 5.5	0.02	0.0155	0	4	5.3–6.1	0.5	155–179	
41	1985 Taiwan (event Lss4), $M_w$ 6.6	0.22	0.236	0	4	5.3–6.1	0.5	155–191	
42	1985 Taiwan (event Lss6), $M_w$ 5.4	0.04	0.03	0	4	5.3–6.1	0.5	155–191	
43	1985 Taiwan (event Lss7), $M_w$ 6.6	0.18	0.193	0	4	5.3–6.1	0.5	155–191	
44	1985 Taiwan (event Lss8), $M_w$ 6.2	0.04	0.038	0	4	5.3–6.1	0.5	155–191	

**Table 1** (continued)

No	Earthquake event, occurrence date and magnitude	PGA (g)	CSR	Number of liquefied sites?		Liquefaction critical depth range (m)	GWT Depth (m)	$V_{s1}$ (m/s)	Cited reference
				Liq.	No liq.				
45	1985 Taiwan (event Lsst12), $M_w$ 6.2	0.18	0.171	0	4	5.3–6.1	0.5	155–191	
46	1985 Taiwan (event Lsst13), $M_w$ 6.2	0.05	0.048	0	4	5.3–6.1	0.5	155–191	
47	1985 Taiwan (event Lsst16), $M_w$ 7.6	0.16	0.230–0.232	0	4	5.3–6.1	0.5	155–191	
48	1989 Loma Prieta, $M_w$ 7	0.13–0.42	0.08–0.287	33	34	2.3–9.9	0.6–6.1	107–222	
49	1993 Kushiro Oki, $M_w$ 8.3	0.41	0.43–0.529	2	0	4.2–4.5	0.9–1.9	135–152	
50	1993 Hokkaido Nanset Oki, $M_w$ 8.3	0.15–0.19	0.184–0.215	3	1	2–7	1–1.4	99–166	
51	1994 Northridge, $M_w$ 6.7	0.51	0.268–0.291	3	0	4.4–5.6	3.4	142–170	
52	1995 Hyogoken Nambu, $M_w$ 6.9	0.12–0.65	0.086–0.455	11	8	3.3–15	1.5–7	126–239	
53	1999 Chi-Chi, $M_w$ 7.6	0.18–0.67	0.113–0.693	18	12	1.35–17.8	0.5–7	128.6–308.5	Saygılı (2005)
54	1999 Kocaeli, $M_w$ 7.4	0.4	0.244–0.434	6	5	1–11	0.77–3.1	103.8–416.6	
55	1999 Chi Chi, $M_w$ 7.6	0.39, 0.67	0.24–0.67	9	3	1.35–11.35	0.5–6.7	129.0–200.0	Chu et al. (2004)

Compared with other aspects of the liquefaction potential evaluation, the uncertainty associated with  $FC$  is relatively minor and thus the influence of  $FC$  on the normalized  $V_{s1}$  was not considered in this study.

**Calibration of  $V_s$ -based liquefaction triggering correlation**

The  $V_s$ -based liquefaction triggering correlation for soil sites was studied herein using the liquefaction analysis framework by Boulanger and Idriss (2012). Specifically, the following liquefaction analysis framework was used in this study: (1) the earthquake-induced cyclic stress ratio ( $CSR$ ) at a given depth of the soil profile was first calculated, and (2) then the cyclic resistance ratio ( $CRR$ ) was computed based on the  $V_{s1}$  of the soil. The liquefaction of soil is said to occur when  $CSR > CRR$ ; otherwise, no soil liquefaction occurs. The  $CSR$  and  $CRR$  are computed at a given depth, which is generally taken at a representative depth of a liquefiable layer at a given test location. The occurrence of liquefaction is based on surface manifestation at the site. Strictly speaking, the exactly one (a set of input data) to one (an observation) correspondence cannot be assured of, as the simplified approach is not about the controlled experimentation. Here,  $CSR$  is expressed as (Idriss and Boulanger 2006; Boulanger and Idriss 2012):

$$CSR = 0.65 \frac{\sigma_v a_{max}}{\sigma'_v g} r_d \frac{1}{MSF K_\sigma} \quad (2)$$

where,  $\sigma_v$  and  $\sigma'_v$  are the vertical total and effective overburden stresses, respectively;  $g$  is the acceleration of gravity;  $a_{max}$  is the maximum horizontal peak ground surface acceleration;  $r_d$  is the shear stress reduction factor;  $MSF$  is the magnitude scaling factor (to adjust all data to  $M_w = 7.5$ ); and  $K_\sigma$  is the overburden correction factor for the cyclic stress ratio ( $K_\sigma = 1.0$  according to Kayen et al. 2013).

The proposed liquefaction triggering correlation between the  $CRR$  and  $V_{s1}$  takes the form of Eq. (3) with five parameters ( $a_1$ – $a_5$ ) in this paper:

$$CRR = \exp \left[ \frac{V_{s1}}{a_1} + \left( \frac{V_{s1}}{a_2} \right)^2 - \left( \frac{V_{s1}}{a_3} \right)^3 + \left( \frac{V_{s1}}{a_4} \right)^4 - a_5 \right] \quad (3)$$

These five parameters could be determined by trial and error using the following two principles: (1) the liquefaction triggering correlation for  $V_{s1} \leq 200$  m/s is generally controlled by the *lower bound* of the liquefaction case history data and (2) the liquefaction triggering correlation for  $V_{s1} > 200$  m/s is generally controlled by the *upper bound* of the non-liquefaction case history data. To further elaborate this point, the parameter  $a_5$  is given a trial value in priori. Four points at the boundary of the liquefaction triggering correlation (marked with larger open circles, as shown in Fig. 2) are then chosen to back-fit the parameters  $a_1$ – $a_4$ . The procedure is



repeated in this trial-and-error procedure to determine the values of parameters  $a_1$ – $a_5$  with an objective of best fitting the boundary that distinguishes regions of high- and low-likelihood of liquefaction occurrence. Therefore, the chance of mistaking a liquefaction case history for a non-liquefaction case history is reduced, thus ensuring that the liquefaction triggering correlation is reasonably conservative. Following these principles, the following equation is obtained:

$$CRR = \exp \left[ \frac{V_{s1}}{86.4} + \left( \frac{V_{s1}}{134.0} \right)^2 - \left( \frac{V_{s1}}{125.2} \right)^3 + \left( \frac{V_{s1}}{158.5} \right)^4 - 4.8 \right] \quad (4)$$

Figure 2 shows the liquefaction triggering correlation given in Eq. (4) along with 618  $V_s$ -based case histories from 49 earthquakes, in which the  $r_d$  and  $M_w$  values from the correlations of Idriss (1999) and Idriss and Boulanger (2006, 2010) are adopted. As seen in Fig. 2, the red triangle plots by Saygili (2005) seem to dominate the location of the boundary curve. These case histories were from the town of Yuanlin during the 1999 Chi-Chi, Taiwan  $M_w$  7.6 earthquake. The town of Yuanlin is located approximately 15 km from the Chelungpu fault rupture. The geometric mean peak ground acceleration (PGA) is 0.18 g. The town is situated on a thick alluvial deposit of the Tsoosui River at the foothill of Baguashan. The ground water table (GWT) is quite shallow, ranging from about 0.5 to 4.0 m below the ground surface. There exist layers of silt fine sand to silty medium fine and very loose sands that are very susceptible to liquefaction (MAA 2000; Juang et al. 2002b). Of the 23 available case histories developed by Green et al. (2011) from the 2010–2011 Christchurch, New Zealand earthquakes, 18 cases indicated surface manifestation of liquefaction, three cases indicated no evidence of

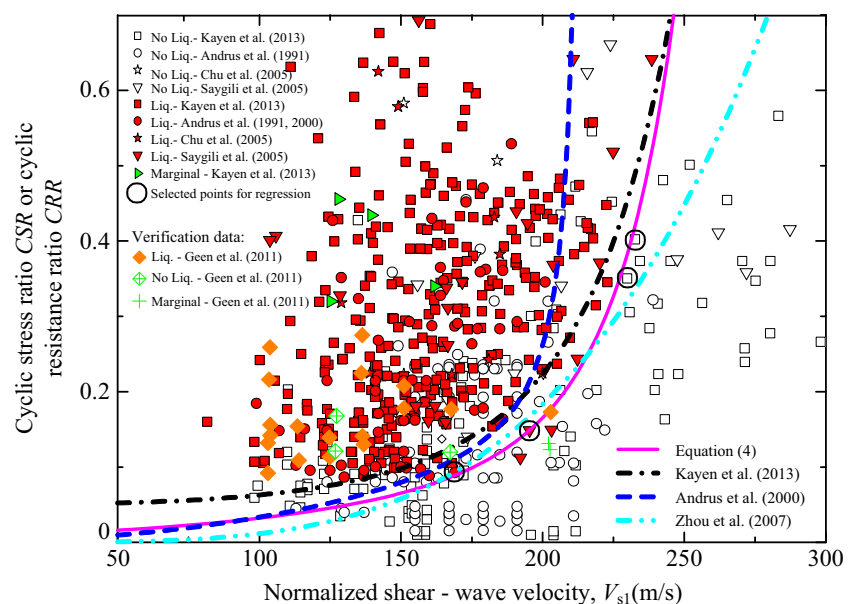
surface manifestation, and three cases were in the margin between liquefaction and non-liquefaction. These cases are not included in the calibration database, and thus provide a more objective way to validate the developed model. These cases are also plotted in Fig. 2, which shows that the predictions by Eq. (4) match well with the observations.

Also shown in this figure are the existing  $V_s$ -based liquefaction triggering correlations developed by Andrus and Stokoe (2000), Zhou and Chen (2007), and Kayen et al. (2013). As shown in Fig. 2, in the region of  $V_{s1} = 95$  to 240 m/s, the liquefaction triggering correlation given in Eq. (4) envelops the liquefaction triggering correlations by Andrus and Stokoe (2000) and Kayen et al. (2013), and appears to be reasonably conservative. On the other hand, unlike the correlation by Zhou and Chen (2007), Eq. (4) is not overly conservative in the high  $V_{s1}$  region ( $V_{s1} > 225$  m/s). Therefore, Eq. (4) is deemed suitable for use in civil engineering projects with high levels of risk potential.

### Sensitivity of the proposed liquefaction correlation to various components of the simplified procedure

All the stress-based simplified approaches for evaluating the liquefaction potential of soil, initiated by Seed and Idriss (1971), are based on an assessment of the  $r_d$  (shear stress reduction factor) of the  $CSR$ . As a result, all existing correlations suffer from moderately biased estimates of in situ  $CSRs$ , especially at shallow depths. Fortunately, the case histories at shallow depth compose a large portion of the database. To this end, three different  $r_d$  models were used to study the effect of different  $r_d$  models on the interpretation of the liquefaction case history database. Figure 3 shows the distribution of the

**Fig. 2**  $V_s$ -based 618 case histories of the liquefaction performance from 49 earthquakes and the verification of the 23 available cases developed by Green et al. (2011) from 2010 to 2011 Christchurch earthquakes



$CSR$  and  $V_{s1}$  of the case history data, in which the  $CSR$  values are computed using three different  $r_d$  models presented by Cetin et al. (2004), Kishida et al. (2009), and Youd et al. (2001), respectively. Also plotted in Fig. 3 is the proposed liquefaction triggering correlation given in Eq. (4). The results shown in Fig. 3 indicate that the position of the proposed liquefaction triggering correlation (Eq. 4), relative to the expanded database, is not sensitive to the formulation of  $r_d$ .

Furthermore, both the magnitude scaling factor ( $MSF$ ) and the shear stress reduction factor  $r_d$  are dependent on the moment magnitude  $M_w$ . However, the  $M_w$  values of the same earthquake events could be assessed somewhat differently in different databases; for example, see Table 2 for the  $M_w$  values of nine earthquake events listed in Idriss and Boulanger (2010) versus those reported in Kayen et al. (2013). The variations in the earthquake magnitude could affect the  $MSF$ , the  $r_d$ , and therefore the  $CSR$ . However, such effect on the position of the proposed liquefaction triggering correlation (Eq. 4), relative to the expanded database, appears to be quite modest, as reflected in Fig. 4, in which the  $M_w$  values from Kayen et al. (2013) and those from Idriss and Boulanger (2010) are adopted.

Similarly, the effect of different formulations of  $MSF$  is examined. Figure 5 shows the proposed liquefaction triggering correlation (Eq. 4) along with the data of  $CSR$  and  $V_{s1}$  of the expanded database, in which  $MSF$  values are computed based on the formulations in Seed and Idriss (1982), Andrus and Stokoe (2000), and Kayen et al. (2013), respectively. Again, the results show that the position of the proposed liquefaction triggering correlation (Eq. 4), relative to the expanded database, is not sensitive to different  $MSF$  formulations.

Finally, the effect of fines content ( $FC$ ) on the proposed liquefaction correlation, relative to the expanded database. Figure 6 shows the proposed liquefaction triggering correlation (Eq. 4) along with the data of  $CSR$  and  $V_{s1}$  for three  $FC$  scenarios,  $FC \leq 5\%$ ,  $5\% < FC \leq 35\%$ , and  $FC > 35\%$ . As can be seen in Fig. 6, the position of the proposed liquefaction correlation (Eq. 4) is quite satisfactory in delineating the liquefaction cases from non-liquefaction cases in all three  $FC$  scenarios. Considering the uncertainty (variation) in the measured  $V_s$  values in the database, which likely out-weights the effect of  $FC$ , it appears adequate to adopt a single liquefaction triggering curve for all  $FC$  scenarios. The liquefaction triggering correlation (Eq. 4) is deemed reasonably and conservatively positioned, relative to the expanded database.

### Mapping function: from nominal safety factor to liquefaction probability

In a deterministic approach, the soil liquefaction is predicted to occur if the factor of safety ( $F_s = CRR/CSR$ ) against the initiation of liquefaction is less than or equal to 1.

Because of the uncertainties existing in the adopted model and the input data, the computed  $F_s$  is a random variable. Juang et al. (2013) used the term “nominal” factor of safety  $\tilde{F}_s$ , a fixed value, which is computed using nominal values of the input parameters. The term “nominal”

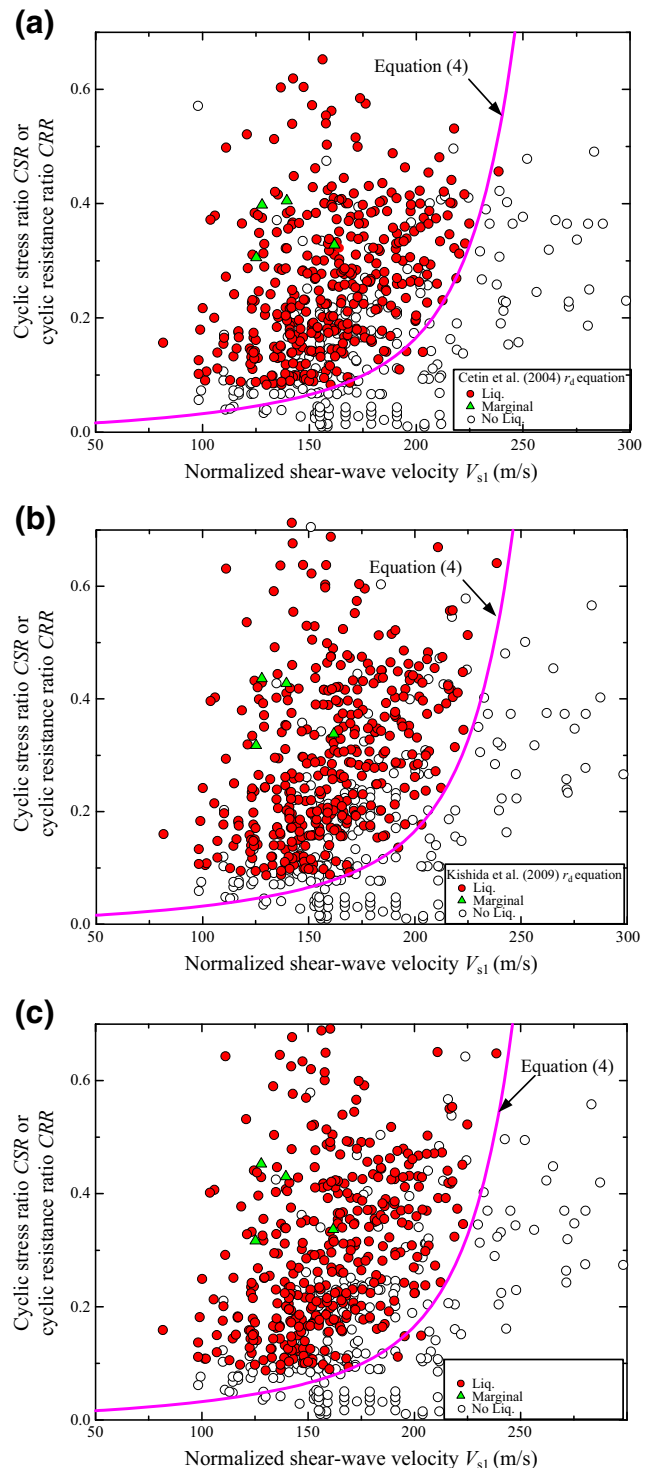


**Fig. 3** The distribution of the liquefaction case history data processed with different  $r_d$  relationships compared to the liquefaction triggering of Eq. (4)

**Table 2** Difference of  $M_w$  values from the databases of Idriss and Boulanger (2010) and Kayen et al. (2013)

Earthquake location, date	$M_w$ from Idriss and Boulanger (2010) database	$M_w$ from Kayen et al. (2013) database
Fukui,1948	7	7.1
Tokachi Oki,1968	7.5	7.9
Tangshan,1976	7.6	8
Aftershock, Nihinkai-Chubu, 1983	6.8	7
Hyogo Nambu,1995	6.9	7
Niigata,1964	7.6	7.5
Haicheng,1975	7	7.1
Miyagi Ken Oki,1978	6.5	6.7
Loma Prieta, 1989	6.93	7

value is used herein as a fixed value estimate of a random variable.

Furthermore, Juang et al. (2002a) suggested a simplified probabilistic model expressed in the form of a mapping function that maps the nominal safety factor ( $\tilde{F}_S$ ) to the probability of soil liquefaction ( $P_L$ ).

$$P_L = \frac{1}{1 + \left(\tilde{F}_S/a\right)^b} \tag{5}$$

where  $a$  and  $b$  are the model parameters.

The model parameters  $a$  and  $b$  may be estimated based on a liquefaction case history database  $D$  with the principle of the maximum likelihood. The weighted likelihood function  $L(a, b|D)$  to account for the data imbalance (i.e., uneven number of liquefaction cases and non-liquefaction cases in a database) using weighting factors  $w_L$  and  $w_{NL}$  may be written as follows (Cetin et al. 2004; Moss et al. 2006; Juang et al. 2012, 2013; Kayen et al. 2013; Chen et al. 2015):

$$L(a, b|D) = \left\{ \prod_{i=1}^{380} \frac{1}{1 + \left(\tilde{F}_S/a\right)^b} \right\}^{w_L} \times \left\{ \prod_{j=1}^{234} \left( 1 - \frac{1}{1 + \left(\tilde{F}_S/a\right)^b} \right) \right\}^{w_{NL}} \tag{6}$$

Here,  $D = \left\{ \left( L^{(i)}, \tilde{F}_S^{(i)} \right); i = 1, \dots, 614 \right\}$ , where  $L^{(i)}$  indicates the  $i$ th case, and  $L^{(i)} = 1$  for the liquefaction case and is 0 otherwise. The values of  $w_L$  and  $w_{NL}$  are the weights assigned to the liquefaction and non-liquefaction cases, respectively.

The adopted global database is dominated by positive liquefaction observations (380 liquefaction cases), with a minority of test sites with no surface manifestation (234

non-liquefaction cases), as depicted in Fig. 2. This unavoidable sampling disparity will result in a bias that may impact the statistical analysis and can produce a skewed

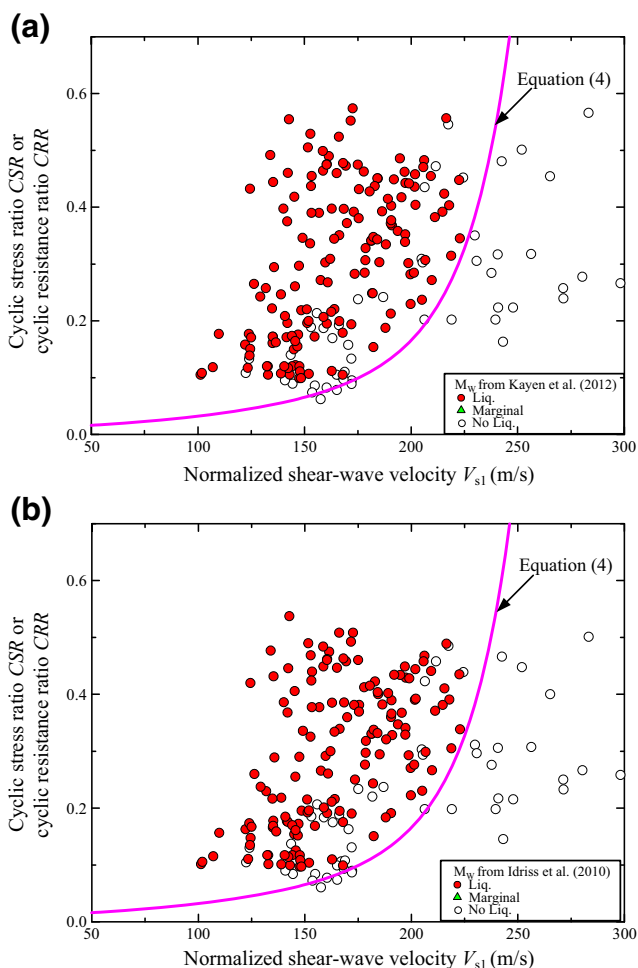


**Fig. 4** Distribution of the liquefaction case history data processed using different moment magnitude  $M_w$  relationships compared to the liquefaction triggering correlation of Eq. (4)



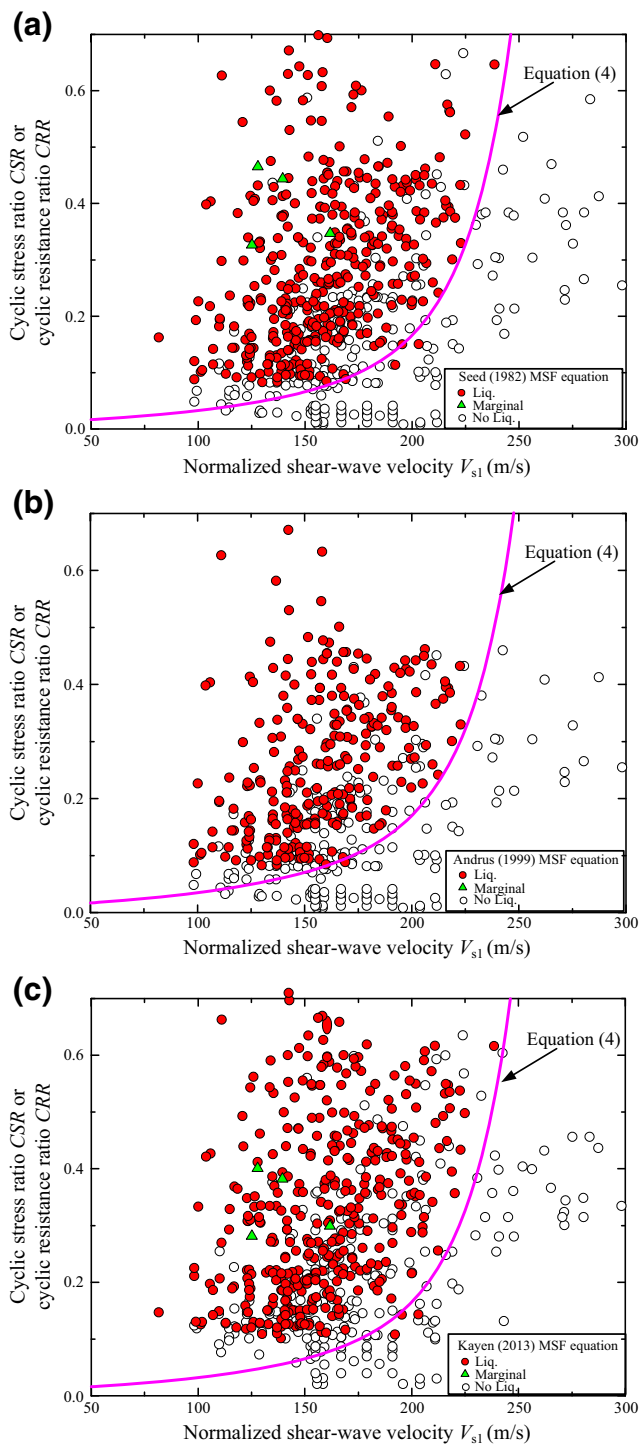


**Fig. 5** Distribution of the liquefaction case history data processed using different MSF relationships compared to the liquefaction triggering correlation of Eq. (4)

prediction, if unchecked (Kayen et al. 2013). In their investigation of this type of bias, Cetin et al. (2004) recommended a methodology to account for this choice-based sampling, and developed a weighting factor ( $w$ ;  $w_{NL}/w_L$ ) for application to the likelihood function of Eq. (6). Based

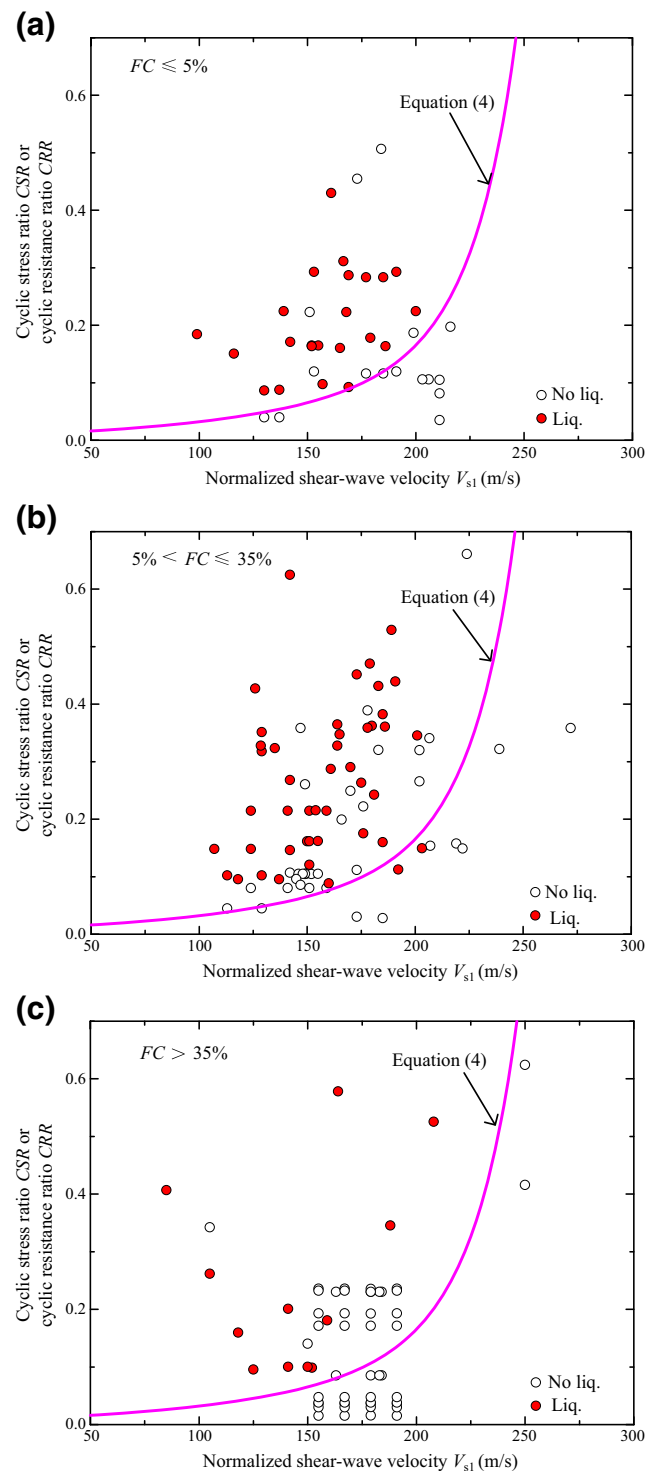


**Fig. 6** Distribution of case history data with different fine contents ( $FC$ ) compared with the liquefaction triggering correlation of Eq. (4)

on the work of Cetin et al. (2004), all “liquefied” data are weighted by a factor of  $w_L = 0.8$ , and all “non-liquefied” data are weighted by a factor of  $w_{NL} = 1.2$ , resulting in a ratio of  $w_{NL}/w_L = 1.5$ .

**Table 3** Parameters  $a$  and  $b$  for Eq. (4) derived using various assumptions of the weight ratios

$w_{NL}/w_L$	$a$	$b$
1.0	0.597	2.532
1.2	0.556	2.519
1.5	0.509	2.511
1.8	0.473	2.508

Intuitively, the weighting factors  $w_L$  and  $w_{NL}$  may be determined based on the number of liquefaction cases and the number of non-liquefaction cases in the database. The number of liquefaction cases is approximately equal to 1.62 times the number of non-liquefaction cases in the adopted database. Based on this intuition, Juang et al. (2013) developed a procedure for estimating the weighting factors, and with the adopted database, the weighting factors are quite consistent with those obtained by Cetin et al. (2004) and Kayen et al. (2013). Therefore, considering the consistency with these previous studies, the weighting factor is adopted as:  $w_{NL}/w_L = 1.5$  ( $w_L = 0.8$  and  $w_{NL} = 1.2$ ) for the adopted global database of case histories. Although the true value of  $w_{NL}/w_L$  is not entirely known, these weighting factors appear to be reasonable. Furthermore, the work of Boulanger and Idriss (2012) suggested that the effect of sampling bias perceived in the database is quite modest.

Using the maximum likelihood procedure described above, the likelihood function based on all 618 cases in the database is maximized to yield the best estimates ( $\tilde{a}, \tilde{b}$ ) of the parameters  $a$  and  $b$  in Eq. (5). The results of the maximum likelihood analysis using different ratios of  $w_{NL}$  to  $w_L$  are listed in Table 3. The models are shown in Fig. 7 in the form of  $P_L = f(\tilde{F}_s)$ . With the adopted  $w_{NL}/w_L = 1.5$ ,  $a = 0.509$  and  $b = 2.511$ , and the relationship between the liquefaction probability  $P_L$  and the nominal safety factor  $\tilde{F}_s$  is expressed as:

$$P_L = \frac{1}{1 + (\tilde{F}_s/0.509)^{2.511}} \tag{7}$$

Alternatively, the  $P_L$ - $\tilde{F}_s$  relationship may be obtained using an empirical approach described in Juang et al. (2013). For each of the 618 cases in the expanded database adopted in this study, the nominal safety factor  $\tilde{F}_s$  is computed using Eqs. (2) and (4). These cases are then placed in different bins based on their  $\tilde{F}_s$  values. Taking a bin width of 0.1 as an example, the first bin covered all cases with  $\tilde{F}_s$  in the range of 0–0.1; the second bin covered all cases with  $\tilde{F}_s$  in the range of 0.1–0.2, and so on. Thus, a set of ( $P_L$ ,  $\tilde{F}_s$ )

data points can be obtained using the weighted empirical probability approach described by Juang et al. (2013), and the empirical relationship of  $P_L$  versus  $\tilde{F}_s$  can be established, as shown in Fig. 7. As shown in Fig. 7, the results of this empirical approach are quite consistent with those obtained with the weighted maximum likelihood technique.

**Probabilistic version of the new  $V_s$ -based liquefaction triggering correlation**

Combining Eqs. (4) and (7) allows the probabilistic version of the calibrated empirical liquefaction triggering correlation of Eq. (4) for the expanded database to be expressed as:

$$CRR = \tilde{F}_s(P_L) \cdot \exp \left[ \frac{V_{s1}}{86.4} + \left( \frac{V_{s1}}{134.0} \right)^2 - \left( \frac{V_{s1}}{125.2} \right)^3 + \left( \frac{V_{s1}}{158.5} \right)^4 - 4.8 \right] \tag{8}$$

where  $\tilde{F}_s(P_L)$  denotes that  $\tilde{F}_s$  is a function of  $P_L$  and its value can be calculated by inverting Eq. (7) for a given  $P_L$ .

According to Eq. (7) and Eq. (8), the deterministic liquefaction triggering correlation of Eq. (4) corresponds to a liquefaction probability of approximately 15%. The liquefaction triggering curves for liquefaction probabilities of 9%, 15%, 25%, 45%, 65%, and 95% based on the expanded database are graphed in Fig. 8. For comparison, the deterministic liquefaction triggering curve recommended by Kayen et al. (2013) is also given in Fig. 8. According to the results shown in Fig. 8, the concept of a limiting upper bound of normalized velocity  $V_{s1}$  (previously set at 215 m/s by Andrus and Stokoe 2000) appears to be inconsistent with the expanded database.

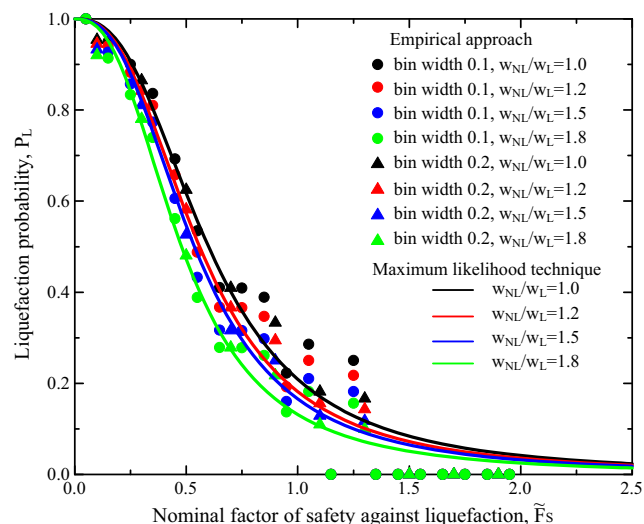
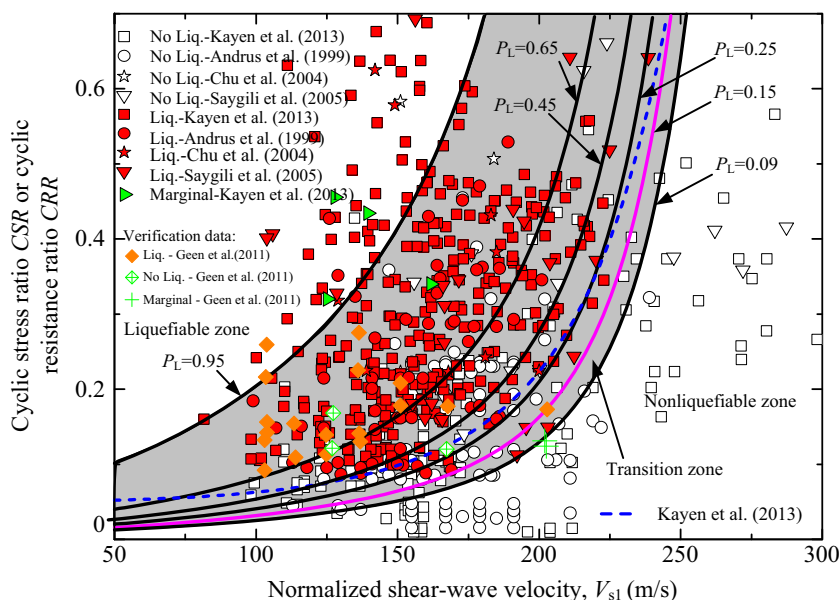


**Fig. 7** Empirical relationship between  $P_L$  and  $\tilde{F}_s$  derived for different values of  $w_{NL}/w_L$  using the weighted maximum likelihood technique and the weighted empirical approach

**Fig. 8** Liquefaction triggering correlations for liquefaction probabilities of 9%, 15%, 25%, 45%, 65%, and 95%, the deterministic liquefaction triggering curve by Kayen et al. (2013) compared to the expanded case history database and the verification of the 23 available cases developed by Green et al. (2011) from 2010 to 2011 Christchurch earthquakes



The deterministic boundary curve of Kayen et al. (2013) is characterized with probabilities ranging from 15% to 45% for  $V_{s1}$  above 115 m/s. Moreover, the intersection of the deterministic boundary curve of Kayen et al. (2013) with the 25% liquefaction probability contour in this study is located approximately at  $V_{s1} = 218$  m/s. The main difference between the two liquefaction triggering curves appears to lie within the region of  $V_{s1}$  below 150 m/s for  $CSR$  below 0.09 and of  $V_{s1}$  approximately 230 m/s above where there are little or no liquefaction case histories. The deterministic boundary curve of Kayen et al. (2013) was also characterized with liquefaction probabilities ranging from 15% to 25% for  $V_{s1}$  above 218 m/s. The newly established deterministic boundary curve (Eq. 4) appears to be slightly more conservative than those recommended in the past studies. However, whether a model is conservative should be viewed in the probability sense. For example, the available cases from the 2010–2011 Christchurch earthquakes (Green et al. 2011) are plotted in Fig. 8 along with the various probability contours. As seen in Fig. 8, some liquefaction cases are located within the liquefaction probabilities ranging from 45% to 65%, one liquefaction case lies on the 15% liquefaction probability contour, and the two margin cases are slightly below the 9% liquefaction probability contour. These results indicate that the newly established deterministic boundary curve and its probability version are quite reasonable.

The zone below the liquefaction triggering correlation for liquefaction probabilities of approximately 9% indicates a non-liquefaction zone for clean sands, the zone above the liquefaction triggering correlation for liquefaction probabilities of 95% indicates a liquefaction zone for clean sands, and the middle gray zone enclosed by the liquefaction triggering correlations for liquefaction probabilities of 9% and 95% is defined as a transition zone for clean sands. The liquefaction

triggering correlations for liquefaction probabilities of 9%, 15%, and 25%, respectively, represent the “very low”, “low”, and “moderate” probability events of mistaking a liquefiable soil for a non-liquefiable soil.

## Conclusions

In this paper, through the use of an expanded database of the  $V_s$ -based liquefaction case histories of Andrus et al. (1999), Chu et al. (2004), Saygili (2005), and Kayen et al. (2013), a new liquefaction triggering correlation equation and its simplified probabilistic version are developed and presented. The following conclusions are drawn:

- (1) The five parameters of the new deterministic liquefaction triggering correlation in Eq. (4) were determined by trial and error using the following two principles: (1) the liquefaction triggering correlation for  $V_{s1} \leq 200$  m/s is generally controlled by the lower bound of the liquefaction case history data and (2) the liquefaction triggering correlation for  $V_{s1} > 200$  m/s is generally controlled by the upper bound of the non-liquefaction case history data. Based on calibration with the expanded database, this deterministic liquefaction triggering correlation (Eq. 4) corresponds to a probability of liquefaction of approximately 15%, which is consistent with those recommended by Cetin et al. (2004), Boulanger and Idriss (2012), and Kayen et al. (2013) for liquefaction triggering correlation.
- (2) The new calibrated liquefaction triggering correlation can envelop the lower bound of the liquefaction triggering correlations published by Andrus and Stokoe (2000), Youd et al. (2001), and Kayen et al. (2013). The new

calibrated liquefaction triggering correlation is reasonably conservative for the expanded database adopted in this paper; the correlation is insensitive to variations in the components of the present simplified liquefaction analysis framework.

- (3) An empirical equation for determining the probability of liquefaction is expressed in the form of a mapping function that maps the nominal factor of safety to the probability of liquefaction. The mapping function, in the form of Eq. (7), obtained by the empirical approach is consistent with that obtained using the weighted maximum likelihood technique.
- (4) A probabilistic version of the new calibrated liquefaction triggering correlation is presented. Based on the probability contour curves, in relation to the expanded database, three zones of liquefaction potential, namely the non-liquefaction, transition, and liquefaction zones, are delineated with liquefaction probabilities of  $\leq 9\%$ ,  $9\%–95\%$ , and  $\geq 95\%$ , respectively. The deterministic liquefaction triggering correlation of Eq. (4), which is generally biased toward the conservative side, corresponds to a liquefaction probability of approximately 15%.

**Acknowledgements** The authors gratefully acknowledge the financial support for this study from the Project of the National Natural Science Foundation of China (51378258, 51438004) and the National Grand Science and Technology Special Project of China (2013ZX06002001-9).

## References

- Ahmadi MM, Paydar NA (2014) Requirements for soil-specific correlation between shear wave velocity and liquefaction resistance of sands. *Soil Dyn Earthq Eng* 57:152–163
- Alba PD, Baldwin K, Janoo V, Roe G, Celikkol B (1984) Elastic-wave velocities and liquefaction potential. *Geotech Test J* 7(2):77–87
- Andrus RD, Stokoe KHII (2000) Liquefaction resistance of soils from shear-wave velocity. *J Geotech Geoenviron Eng ASCE* 126(11):1015–1025
- Andrus RD, Stokoe KHII, Chung RM (1999) Draft guidelines for evaluating liquefaction resistance using shear wave velocity measurements and simplified procedures. US Depart Comm, Technol Admin, Ntnl Inst Stand Technol
- Andrus RD, Stokoe KHII, Juang CH (2004) Guide for shear wave-based liquefaction potential evaluation. *Earthquake Spectra* 20(2):285–308
- Bhattacharya S, Hyodo M, Goda K, Tazoh T, Taylor CA (2011) Liquefaction of soil in the Tokyo Bay area from the 2011 Tohoku (Japan) earthquake. *Soil Dyn Earthq Eng* 31(11):1618–1628
- Boulanger RW, Idriss IM (2012) Probabilistic standard penetration test-based liquefaction-triggering procedure. *J Geotech Geoenviron Eng ASCE* 138(10):1185–1195
- Cetin KO, Kiureghian AD, Seed RB (2002) Probabilistic models for the initiation of seismic soil liquefaction. *Struct Saf* 24(1):67–82
- Cetin KO, Seed RB, Kiureghian AD, Tokimatsu K, Harder LF, Kayen RE, Moss RES (2004) Standard penetration test-based probabilistic and deterministic assessment of seismic soil liquefaction potential. *J Geotech Geoenviron Eng ASCE* 130(12):1314–1340
- Chen Y, Ke H, Chen R (2005) Correlation of shear wave velocity with liquefaction resistance based on laboratory tests. *Soil Dyn Earthq Eng* 25(6):461–469
- Chen GX, Xu LY, Kong MY, Li XJ (2015) Calibration of a CRR model based on an expanded SPT-based database for assessing soil liquefaction potential. *Eng Geol* 196:305–312
- Chu BL, Hsu SC, Chang YM (2004) Ground behavior and liquefaction analyses in central Taiwan-Wufeng. *Eng Geol* 71(1):119–139
- Dabiri R, Askari F, Shafiee A, Jafari MK (2011) Shear wave velocity-based liquefaction resistance of sand-silt mixtures: deterministic versus probabilistic approach. *Iranian journal of science and technology. Trans Civil Eng* 35(C2):199–225
- Dobry R, Ladd RS, Yokel FY, Chun RM, Powell D (1982) Prediction of pore water pressure buildup and liquefaction of sands during earthquakes by the cyclic strain method. National Bureau of Standards Building Sci. Ser, U.S., 138, Washington, DC
- Dobry R, Abdoun T, Stokoe KHII, Moss RES, Hatton M, El Ganainy H (2015). Liquefaction Potential of Recent Fills versus Natural Sands Located in High-Seismicity Regions Using Shear-Wave Velocity. *J Geotech Geoenviron Eng ASCE* 141(3): [https://doi.org/10.1061/\(ASCE\)GT.1943-5606.0001239](https://doi.org/10.1061/(ASCE)GT.1943-5606.0001239)
- Elgamal A, Zeghal M, Parra E (1996) Liquefaction of reclaimed island in Kobe, Japan. *J Geotech Eng ASCE* 122(1):39–49
- Fu SC, Tatsuoka F (1984) Soil liquefaction during Haicheng and Tangshan earthquake in China: a review. *Soils Found* 24(4):11–29
- Green RA, Wood C, Cox B, Cubrinovski M, Witherspoon L, Bradley B, Algie T, Allen J, Bradshaw A, Rix G (2011) Use of DCP and SASW tests to evaluate liquefaction potential: predictions vs. observations during the recent New Zealand earthquakes. *Seismol Res Lett* 82(6):927–938
- Huang YT, Huang AB, Kuo YC, Tsai MD (2004) A laboratory study on the undrained strength of a silty sand from central western Taiwan. *Soil Dyn Earthq Eng* 24(9):733–743
- Idriss IM (1999) An update to the Seed-Idriss simplified procedure for evaluating liquefaction potential. In: Proceedings of the TRB Workshop on New Approaches to Liquefaction, Publication No. FHWARD-99-165, Federal Highway Administration, Washington, DC
- Idriss IM, Boulanger RW (2006) Semi-empirical procedures for evaluating liquefaction potential during earthquakes. *Soil Dyn Earthq Eng* 26(2):115–130
- Idriss IM, Boulanger RW (2008) Soil Liquefaction during Earthquakes. Monograph MNO-12, Earthquake Engineering Research Institute, Oakland, p 261
- Idriss IM, Boulanger RW (2010) SPT-based liquefaction triggering procedures. Report UCD/CGM-10/02, Department of Civil and Environmental Engineering, University of California, Davis
- Iwasaki T, Tatsuoka F (1977) Effects of grain size and grading on dynamic shear moduli of sands. *Soils Found* 17(3):19–35
- Juang CH, Chen CJ, Jiang T (2001) Probabilistic framework for liquefaction potential by shear wave velocity. *J Geotech Geoenviron Eng ASCE* 127(8):670–678
- Juang CH, Jiang T, Andrus RD (2002a) Assessing probability based methods for liquefaction evaluation. *J Geotech Geoenviron Eng ASCE* 128(7):580–589
- Juang CH, Yuan H, Lee DH, Ku CS (2002b) Assessing CPT-based methods for liquefaction evaluation with emphasis on the cases from the chi-chi, Taiwan, earthquake. *Soil Dyn Earthq Eng* 22(3):241–258
- Juang CH, Yang SH, Yuan H (2005) Model uncertainty of shear wave velocity-based method for liquefaction potential evaluation. *J Geotech Geoenviron Eng ASCE* 131(10):1274–1282
- Juang CH, Ching J, Luo Z, Ku CS (2012) New models for probability of liquefaction using standard penetration tests based on an updated database of case histories. *Eng Geol* 133-134:85–93
- Juang CH, Ching J, Luo Z, Ku CS (2013) Assessing SPT-based probabilistic models for liquefaction potential evaluation: a 10-year update. *Georisk* 7(3):1–14



- Kayen RE, Mitchell JK, Seed RB, Lodge A, Nishio S, Coutinho RQ (1992). Evaluation of SPT-, CPT-, and shear wave-based methods for liquefaction potential assessment using Loma Prieta Data. In: Proceedings of the 4th US-Japan Workshop on Earthquake Resistant Design of Lifeline Facilities and Countermeasures for Soil Liquefaction, NCEER-92-0019. National Center for Earthquake Engineering Research, Buffalo, N.Y.; 1992:177–92
- Kayen R, Moss RES, Thompson EM, Seed RB, Cetin KO, Kiureghian AD, Tanaka Y, Tokimatsu K (2013) Shear-wave velocity-based probabilistic and deterministic assessment of seismic soil liquefaction potential. *J Geotech Geoenviron Eng ASCE* 139(3):407–419
- Kishida T, Boulanger RW, Abrahamson NA, Driller MW, Wehling TM (2009) Site effects for the Sacramento-san Joaquin Delta. *Earthquake Spectra* 25(2):301–322
- Liu H (1986) Seismic damage during Tangshan great earthquake (vol. 1). Seismology Press, Beijing (in Chinese)
- Liu N, Mitchell JK (2006) Influence of nonplastic fines on shear wave velocity-based assessment of liquefaction. *J Geotech Geoenviron Eng ASCE* 132(8):1091–1097
- Lodge AL (1994). Shear wave velocity measurements for subsurface characterization. Ph.D. thesis, University of California, Berkeley
- MAA (2000) Soil liquefaction assesment and remediation study, paase I (Yuanlin, Dachun, and Shetou), summary report and appendixes. Moh and Associates, Taipei (in Chinese)
- Moss RES (2008) Quantifying measurement uncertainty of thirty-meter shear-wave velocity. *Bull Seismol Soc Am* 98(3):1399–1411
- Moss RES, Seed RB, Kayen RE, Stewart JP, Kiureghian AD, Cetin KO (2006) CPT-based probabilistic and deterministic assessment of in situ seismic soil liquefaction potential. *J Geotech Geoenviron Eng ASCE* 132(8):1032–1051
- Polito CP (1999). The effect of non-plastic and plastic fines on the liquefaction of sandy soils. Ph.D. thesis, Virginia Polytechnic Institute and State University, Blacksburg
- Quigley MC, Bastin S, Bradley BA (2013) Recurrent liquefaction in Christchurch, New Zealand, during the Canterbury earthquake sequence. *Geology* 41(4):419–422
- Research Group for Hazard of Niigataken Chuetsu-oki Earthquake (2008). The Niigataken Chuetsu-oki Earthquake in 2007, the Association for the Geological Collaboration in Japan (in Japanese)
- Robertson PK, Woeller DJ, Finn WDL (1992) Seismic cone penetration test for evaluating liquefaction potential under cyclic loading. *Can Geotech J* 29(4):686–695
- Saygili G (2005). Liquefaction potential assessment in soil deposits using artificial neural networks. Ph.D. thesis, Concordia University
- Seed HB (1979) Soil liquefaction and cyclic mobility evaluation for level ground during earthquakes. *J Geotech Eng Div ASCE* 105(2):201–255
- Seed HB (1987) Design problems in soil liquefaction. *J Geotech Eng ASCE* 113(8):827–945
- Seed HB, Idriss IM (1971) Simplified procedure for evaluating soil liquefaction potential. *J Soil Mech Found Div ASCE* 97(SM9):1249–1273
- Seed HB, Idriss IM (1982) Ground motions and soil liquefaction during earthquakes (Vol. 5). Berkeley, Earthquake Engineering Research Institute, University of California
- Seed HB, Tokimatsu K, Harder LF, Chung RM (1985) Influence of SPT procedures in soil liquefaction resistance evaluations. *J Geotech Eng ASCE* 111(12):1425–1445
- Tokimatsu K, Uchida A (1990) Correlation between liquefaction resistance and shear wave velocity. *Soils Found* 30(2):33–42
- Uyanik O, Taktak AG (2009) A new method for liquefaction analysis from shear wave velocity and predominant resonance period. *J Nat Appl Sci* 13(1):74–81
- Yamaguchi A, Mori T, Kazama M, Yoshida N (2012) Liquefaction in Tohoku district during the 2011 off the pacific coast of Tohoku earthquake. *Soils Found* 52(5):811–829
- Youd TL, Idriss IM, Andrus RD, Arango I, Castro G, Christian JT, Dobry R, Finn WDL, Harder LF, Hynes ME, Ishihara K, Koester JP, Liao SSC, Marcuson IIIWF, Martin GR, Mitchell JK, Moriwaki Y, Power MS, Robertson PK, Seed RB, Stokoe KHII (2001) Liquefaction resistance of soils: summary report from the 1996 NCEER and 1998 NCEER/NSF workshops on evaluation of liquefaction resistance of soils. *J Geotech Geoenvironmen Eng ASCE* 127(10):817–833
- Zhou YG, Chen YM (2007) Laboratory investigation on assessing liquefaction resistance of sandy soils by shear wave velocity. *J Geotech Geoenviron Eng ASCE* 133(8):959–972
- Zhou YG, Chen YM, Shamoto Y (2010) Verification of the soil-type specific correlation between liquefaction resistance and shear-wave velocity of sand by dynamic centrifuge test. *J Geotech Geoenviron Eng ASCE* 136(1):165–177